

CLASH: Collision Learning via Augmented Sim-to-real Hybridization to Bridge the Reality Gap

Haotian He¹, Ning Guo², Siqi Shi³, Qipeng Liu², Wenzhao Lian^{2,†}

Abstract—The sim-to-real gap, particularly in the inaccurate modeling of contact-rich dynamics like collisions, remains a primary obstacle to deploying robot policies trained in simulation. Conventional physics engines often trade accuracy for computational speed, leading to discrepancies that prevent direct policy transfer. To address this, we introduce Collision Learning via Augmented Sim-to-real Hybridization (CLASH), a data-efficient framework that creates a high-fidelity hybrid simulator by learning a surrogate collision model from a minimal set of real-world data. In CLASH, a base model is first distilled from an imperfect simulator (MuJoCo) to capture general physical priors; this model is then fine-tuned with a remarkably small number of real-world interactions (as few as 10 samples) to correct for the simulator’s inherent inaccuracies. The resulting hybrid simulator not only achieves higher predictive accuracy but also reduces collision computation time by nearly 50%. We demonstrate that policies obtained with our hybrid simulator transfer more robustly to the real world, doubling the success rate in sequential pushing tasks with reinforcement learning and significantly increase the task performance with model-based control.

I. INTRODUCTION

In recent years, simulation environments have seen explosive growth in capability, becoming a cornerstone of robotic strategy development. Unlike empirical data collection in the real world, which is often costly, time-consuming, and poses safety risks, training in simulation allows for rapid and scalable generation of diverse experiences in a controlled, risk-free setting[1]. This efficiency and safety make simulators indispensable for pretraining complex policies before deployment on physical systems. Modern engines such as MuJoCo[2] can capture rich rigid-body and contact dynamics, while GPU-parallel platforms like NVIDIA Isaac Lab[3] make it feasible to train at massive scale with thousands of synchronized environments. These simulators provide a low-cost way to train a preliminary policy with state-of-art reinforcement learning algorithms like PPO[4] or SAC[5]. However, the “sim-to-real” gap, stemming from unmodeled effects, sensing latencies, inaccurate identified parameters and other mismatches, often prevents policies learned in simulation from transferring directly to physical robots.

Among various physical processes, collisions are particularly challenging to simulate accurately due to their discontinuous nature and sensitivity to frictional effects. Formally, rigid-body collisions with friction are governed by non-linear complementarity problems (NCPs)[6], which are hard to solve both accurately and efficiently. To maintain real-time

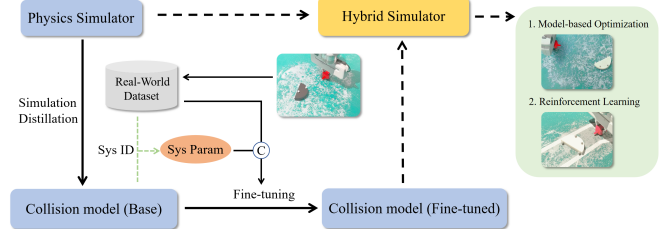


Fig. 1: Overview of our CLASH framework and learning downstream tasks with the hybrid simulator.

performance, many simulators[7], [8], [9], [10] adopt various relaxations and approximations, such as penalty-based contacts or linearized friction cones. While computationally efficient, these relaxations often introduce errors in angular velocity change, frictional dissipation, and post-impact trajectories. Since many manipulation tasks such as pushing or striking rely critically on collision dynamics, reducing this sim-to-real gap in collision modeling is essential.

To mitigate sim-to-real gap mentioned above, many methods are proposed such as improving system identification[11], [12], [13], [14], domain randomization[15], domain adaptation[16] or augmenting simulators with learned models[17], [18], [19], [20]. However, directly learning an augmented model often requires large amount of real-world data. To improve data-efficiency, we can first pre-train a neural surrogate model with simulation data to approximate the dynamics of the simulator. This can be viewed as a form of distillation from the physics engine, where the implicit physical priors are transferred into a differentiable model. Then we fine-tune the model on a few real interactions to compensate for the imperfections and computational shortcuts of the physics engine.

Building on this insight, we introduce a hybrid simulation framework and choose collision dynamics as the representative use case to demonstrate the learning procedure. Specifically, we propose our framework named Collision Learning via Augmented Sim-to-real Hybridization (CLASH) as shown in Fig. 1. The hybrid simulator is not only more accurate than the traditional simulator MuJoCo, but also significantly reduces the computation time associated with collision calculation.

Our contribution can be summarized as follows:

- We introduce CLASH, a data-efficient framework that distills physical priors from simulation and adapts them with limited real-world data, enabling a surrogate col-

¹School of Mathematical Sciences, Peking University. ²School of Artificial Intelligence, Shanghai Jiao Tong University. ³School of Mathematical Sciences, Beijing Normal University. [†]Corresponding Author.

lision model that predicts contact dynamics more faithfully than standard physics engines.

- We develop a hybrid simulator that seamlessly integrates the surrogate model with MuJoCo, achieving both higher accuracy in collision outcomes and reduced computational cost for simulation.
- We demonstrate that this hybrid simulator enhances downstream robot learning, showing consistent gains in both model-based control and reinforcement learning tasks, narrowing the sim-to-real gap and improving real-world task success.

II. RELATED WORK

A. Physics Simulator

Recent years, various physics simulators provide high-performance, realistic rigid-body dynamics and contact modeling optimized for robotics, biomechanics, and reinforcement learning[2], [3], [21], [7], [22]. MuJoCo[2] delivers efficient and accurate contact dynamics and actuator modeling and provides a basic platform for reinforcement learning training. Meanwhile, engines like Isaac Lab[3] support GPU-accelerated, parallelized simulation environments tailored for large-scale RL training. It also provides photo-realistic scenes rendering for users to check the policy execution results. RoboVerse [22] builds a unified robotic learning framework that integrates multiple simulators to enhance sim-to-real transfer. These platforms excel in computational speed, stability, and community adoption, but lack native support for automatic differentiation, making them less suitable for gradient-based system identification or data-efficient learning.

To utilize gradient information, physics simulators, such as TDS[17], MJX[23], Warp[24] and GradSim[25], enable end-to-end differentiation through physical dynamics, contact, and sometimes rendering. MJX[23] reimplements MuJoCo’s dynamics in JAX, delivering differentiable simulation with GPU acceleration. GradSim[25] combines differentiable multi-physics with differentiable rendering, facilitating visuomotor control and system identification directly from images. Although these frameworks empower gradient-based optimization, they often face challenges in terms of performance efficiency, numerical stability, or modeling fidelity—especially for complex, contact-rich physical interactions.

B. Contact Modeling

Contact dynamics in rigid-body simulation is often formulated as a nonlinear complementarity problem (NCP)[6]. However, solving NCPs can be computationally expensive and prone to numerical instability, especially in complex contact scenarios. To achieve efficient and stable simulation, modern physics engines typically introduce various relaxations to the original problem. A typical approach is to approximate the nonlinear second-order friction cone with a linearized cone, thereby reducing the problem to a linear complementarity problem (LCP)[9], [7], [10]. However, this relaxation may cause a misalignment between the

contact friction force and the true velocity direction. Another widely used strategy is to soften the complementarity constraints, effectively replacing hard contacts with penalty-based compliant contacts[2], [9]. While computationally efficient, this approach inevitably introduces non-physical penetration. These relaxations reflect a fundamental trade-off between accuracy and efficiency. Despite the resulting sim-to-real discrepancies, modern simulators generally provide a useful approximation of post-impact states, which can subsequently be corrected with real-world data.

C. Closing the Sim2real Gap

A common strategy to close the sim-to-real gap is Domain Randomization[15], which exposes policies to a wide range of simulated environmental and physical variations during training. But the method is limited if the policy strongly relies on the environmental parameters. Another useful method is domain adaptation[16], which aligning features or visual representations in simulation to real world to mitigate the gap.

Accurate parameter identification is another common approach to build a simulation environment that is closer to reality. [12] uses Warp[24], a differentiable simulator and robot proprioception to deduce object parameters. [11] trains an exploration policy to interact with the object and estimates the parameters while [13] builds a Real-to-Sim-to-Real loop framework and updates estimated parameters iteratively. The most relative one to our work is [14], which trains a surrogate model with simulators to identify parameters. However, they still infer the future states with physics simulators rather than the surrogate model, thus fail to eliminate complex, unmodeled effects that cannot be captured by tuning a fixed set of physical parameters.

Beyond system identification, augmenting simulators with neural networks has emerged as a prominent direction to compensate for unmodeled effects. For example, [18] learns the residual dynamics between simulation and the real world to improve policy transfer, though the model bias may hinder efficient learning. Another line of work directly leverages data-driven models: [26] employs an LSTM to correct policies trained in simulation, while [19] further models the sim-to-real gap and its uncertainty using variational recurrent neural networks. [17] incorporates a differentiable simulator to identify system parameters and neural networks are trained to model the residual effects. However, unstable gradients in contact-rich scenarios limit the broader applicability of this framework. To extend the idea of augmenting simulators with learned models to a wider range of engines while requiring only limited real-world data, we propose our novel framework.

III. METHOD

A. System Overview

In this section, we present an overview of our framework, Collision Learning via Augmented Sim-to-real Hybridization (CLASH), as illustrated in Fig. 2. Since collision dynamics are among the least accurately modeled components

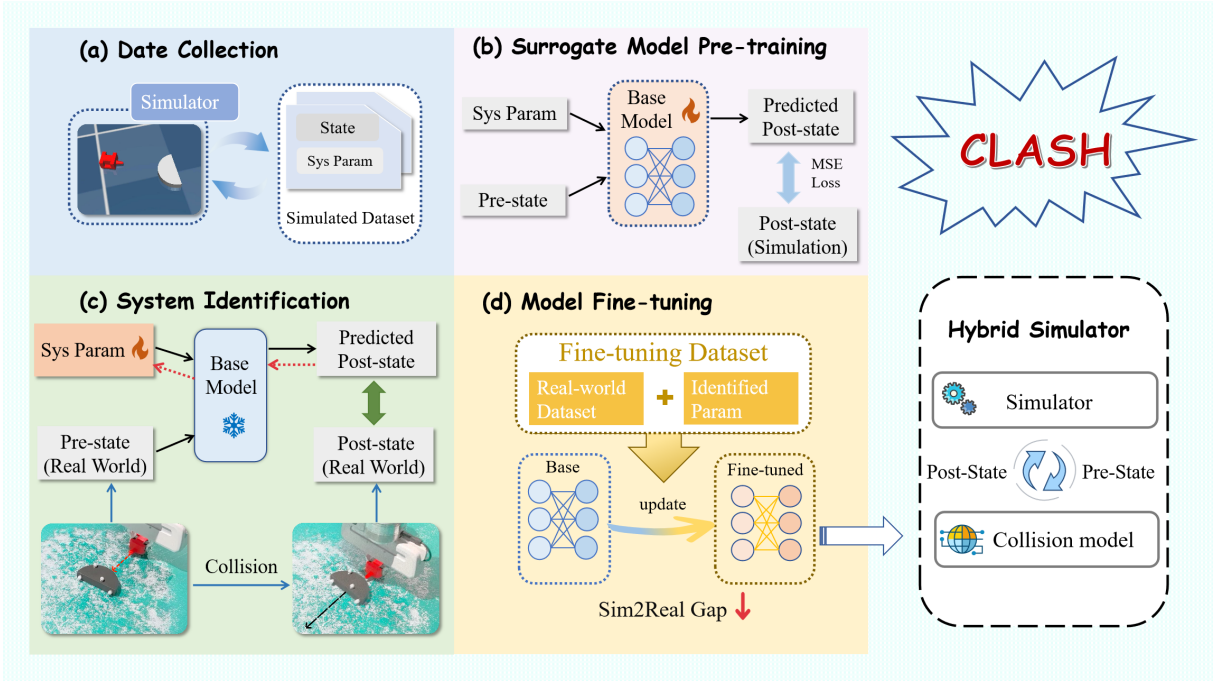


Fig. 2: Our framework Collision Learning via Augmented Sim-to-real Hybridization (CLASH): First collect collision dataset from physics simulator and pre-train a base model to learn the collision dynamics, then adopt the model to identify the system parameters for real-world collision. Subsequently, fine-tune with real-world dataset to obtain a collision model. Finally, integrate the collision model with the physics simulator to build a hybrid simulator that is close to reality.

in physics simulators, we enhance this part by replacing it with a neural network. We define collisions as short-duration impulsive contacts between objects, in contrast to continuous sliding interactions on a tabletop. When collisions take place with ground contact maintained, we model post-impact velocities as the combined outcome of object-object impulse and ground reaction.

We adopt a three-stage procedure to build our neural network-based simulator for data efficiency and high fidelity. Initially, a surrogate base model is pre-trained on extensive simulated dataset, effectively distilling the general physical priors of the simulation engine into a differentiable representation. Subsequently, this base model is fine-tuned using a sparse set of real-world observations to correct for sim-to-real discrepancies. Finally, CLASH produces a hybrid simulator that dynamically offloads computation to the fine-tuned neural network whenever a collision is detected. By grounding the simulator on real-world data, it yields collision dynamics with significantly higher physical fidelity than the original physics-based simulation. This high-fidelity environment can then be employed for a variety of downstream tasks, enabling the training of reinforcement learning policies and the direct application of model-based optimization algorithms to discover effective actions.

B. Training Surrogate Base Model

We denote the system parameters as $P = (\mu, e)$, where μ is the vector of friction coefficients and e represents the damping ratio from MuJoCo’s solref parameter, which

controls the restitution behavior in collisions. Both vectors include values for object-object contacts as well as for object-ground contacts. Given two geometry meshes to collide, we randomly set experimental parameters P , collision velocity and impact point. Then we define the pre-collision state S_{pre} according to the chosen velocity and impact point. The physics simulator then executes the collision process and outputs the corresponding post-collision state S_{post} :

$$S_{post} = \text{Sim}(S_{pre}, P). \quad (1)$$

By repeating this procedure, we collect a dataset of collision pairs (S_{pre}, P, S_{post}) , which constitutes the simulation dataset D_{sim} . A surrogate base model $f_{\theta}(S_{pre}, P)$ is then trained to capture the collision dynamics for the given meshes. The model takes the pre-collision state and system parameters as input and predicts the post-collision state. Since our focus is on the mapping from velocities before and after the collision rather than the full transient process, we parameterize f_{θ} as a three-layer multilayer perceptron (MLP). The model is optimized by minimizing the mean squared error (MSE) between the predicted and simulated post-collision states:

$$\mathcal{L}_{base} = \frac{1}{|D_{sim}|} \sum_{(S_{pre}, P, S_{post}) \in D_{sim}} \|f_{\theta}(S_{pre}, P) - S_{post}\|^2. \quad (2)$$

This surrogate model approximates the non-linear collision dynamics with a differentiable neural network. Although the model can accurately predict post-collision states within the simulator, it inevitably inherits the simulator’s modeling

and numerical errors. Therefore, additional real-world data are required to further adapt the model and enable reliable predictions for real-world collisions.

C. System Identification And Fine-tuning

To adapt the base model to real-world scenarios, we first collect collision data $D_{real} = \{(S_{pre}, S_{post})\}$ with a motion capture system. Before fine-tuning the base model, we need to identify the system parameters. When collecting data from a real scene, we assume that the parameters remain constant to maintain consistency for system identification. Since the motion capture data include complete sliding trajectories, for simplicity, the friction coefficients between objects and the ground are efficiently determined using linear regression. For the remaining parameters, we leverage the differentiable simulation-distilled base model. With frozen weights in the model, we optimize the system parameters to minimize the MSE loss:

$$\mathcal{L}_{sys} = \frac{1}{|D_{real}|} \sum_{(S_{pre}, S_{post}) \in D_{real}} \|f_{\theta}(S_{pre}, P) - S_{post}\|^2. \quad (3)$$

Here f_{θ} is a MLP, so we can apply gradient-based optimization to efficiently obtain the optimal parameters.

The identified parameters $P_{real} := \arg \min_P \mathcal{L}_{sys}$ can be directly used in the physics simulator, as done in [14]. But to further leverage real-world collision data and reduce the sim-to-real gap, we additionally fine-tune the surrogate base model using D_{real} with P_{real} fixed. To avoid overfitting, we perform small-step and early-stopped gradient updates (e.g., 10 iterations). Conceptually, this adaptation learns data-driven residuals that capture unmodeled real-world effects (e.g., subtle frictional dissipation and compliance). The fine-tuned model remains faithful to the original simulator’s structure prior, yet achieves measurably higher accuracy in the real world.

D. Hybrid Simulator

After the two steps above, we obtain a collision model capable of predicting the post-collision state in the real world from a given pre-collision state. We integrate this learned collision model into a physics simulator, replacing the default collision computation, to create a hybrid simulator. The simulator switches to the neural network to predict the post-collision state whenever a collision between two meshes is detected. This plug-and-play design allows seamless integration of the collision model into existing simulators with minimal modification.

As illustrated in Fig. 3a, this high-fidelity hybrid simulator can be directly employed in the two main paradigms: model-based optimization and reinforcement learning (RL). First, the simulator’s accuracy allows gradient-free optimization algorithms like Cross-Entropy Method (CEM)[27] and Covariance Matrix Adaptation Evolution Strategy (CMA-ES)[28] to discover effective open-loop control inputs that successfully transfer to the physical system for single-shot manipulation tasks. This is analogous to calculating the precise force and angle for a golf or billiard shot to achieve a desired outcome.

Second, the hybrid simulator provides a physically plausible training environment that significantly improves sim-to-real policy transfer for RL. As our experiments confirm, utilizing such an accurate simulator in SAC training directly leads to policies that transfer more reliably to a real-world executions.

IV. EXPERIMENTS

In this section, we present a series of experiments to demonstrate the effectiveness of the proposed CLASH framework. We first evaluate the prediction accuracy of the collision model trained in CLASH. Then, we construct a hybrid simulator as described in Section III-D and apply it to two representative downstream tasks:

- finding the best control signal to hit a block given the target position and orientation,
- training a policy with reinforcement learning to repeatedly hit a block until it reaches the target.

These two tasks are chosen to cover both planning-based control and learning-based control paradigms. The first task highlights how the hybrid simulator can directly support model-based search for optimal actions in a single-shot hitting scenario, while the second task examines whether the improved simulator facilitates the training of robust RL policies in sequential decision-making settings.

For the simulation experiments, we adopt MuJoCo as the physics simulator since it provides the most accurate collision simulation. For real-world experiments, we use a 7-DOF Franka robotic arm to grab the impact block and hit the target block. The robot is controlled using the native libfranka C++ library in Cartesian velocity control mode. The data is recorded by a motion capture (MoCap) system with 16 cameras. The overall experimental setup is illustrated in Fig. 3b.

A. Learning Collision Model

To build a hybrid simulator, we first need to train a collision model following CLASH framework. We 3D-print a customized impact block and grab it with the Franka robotic arm to strike various stationary objects. For the target object, we primarily choose a semi-cylinder, since its anisotropic geometry makes the collision outcome highly sensitive to the impact point.

1) *Data and Training Details:* In simulation, we generate 100,000 collision data pairs in MuJoCo by varying pre-collision states and system parameters. The sampling ranges of all parameters are summarized in Table I. In real-world experiments, we consider three materials for the target object (resin, nylon, and PETG-CF) and two types of sand (high-friction and low-friction) sprinkled evenly on the table surface to simulate diverse contact environments. For each material–surface setting, we collect 110 collision samples from different impact angles. Among them, the first 10 samples (denoted as D_{train}) are used for parameter identification and fine-tuning, while the remaining 100 samples (denoted as D_{test}) are reserved for evaluation. We use a three-layer MLP with hidden layer width of 128 and ReLU activations. We first pretrain the base model on simulated data for 1,000

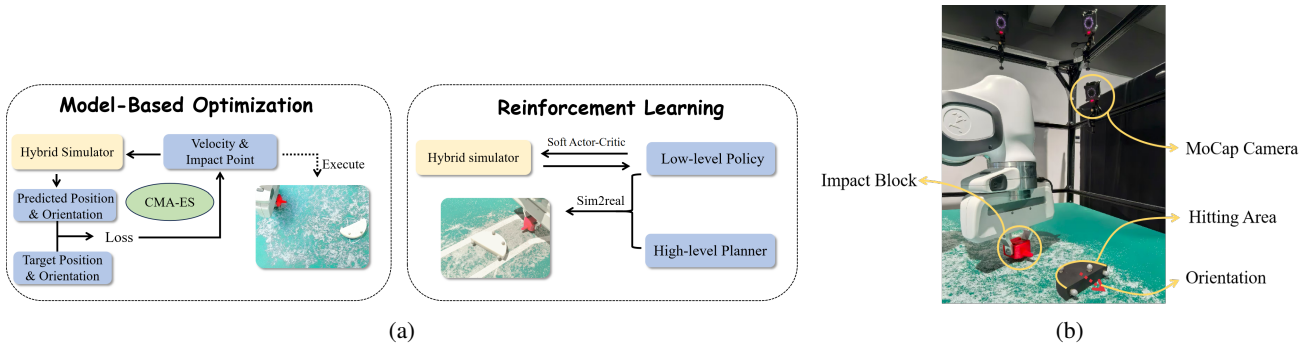


Fig. 3: (a) The proposed hybrid simulator is applied to two downstream tasks: model-based optimization and reinforcement learning. (b) System setup, where a Franka arm manipulates an impact block to strike the semi-cylinder block.

TABLE I: Simulation Settings

Symbol	Definition	Range
v_{pre}	Velocity before collision	[0.2, 0.8]
θ	Deflection angle of the impact point relative to the center of the semicircle	$[\frac{\pi}{12}, \frac{11\pi}{12}]$
θ_1	Deflection angle of the velocity relative to the impact point	$[-\frac{\pi}{12}, \frac{\pi}{12}]$
μ_1	Friction coefficient between impact block and semi-cylinder	[0.05, 1]
μ_2	Friction coefficient between ground and semi-cylinder	[0.02, 1]
e_1	Damping ratio between impact block and semi-cylinder	[0.1, 3]
e_1	Damping ratio between ground and semi-cylinder	[0.1, 3]

optimization steps. On real data, we then perform two-stage adaptation: (i) environment parameters are optimized for 1,000 steps with the base network frozen, and (ii) the base model is unfrozen and fine-tuned for 10 steps. All training employs the AdamW[29] optimizer with a learning rate of 0.001 and weight decay of 0.01.

2) *Methods and Metrics*: We compare our collision model against three baselines. The first baseline uses MuJoCo, which is non-differentiable. We estimate system parameters via grid search on real-world data and then simulate the collision process in MuJoCo. The second baseline employs the differentiable simulator MJX[23]. The third baseline directly fits a neural network on 10 real-world collision samples without pre-training on simulation data. For evaluation, we define prediction accuracy based on a relative error threshold. Specifically, let D_α denotes the subset of the test set D_{test} in which the relative error between the predicted post-collision state and the ground-truth state is smaller than α . The prediction accuracy is then defined as:

$$\text{Accuracy}(\alpha) = \frac{|D_\alpha|}{|D_{test}|} \quad (4)$$

3) *Results*: As shown in Fig. 4, our model consistently outperforms the three baselines across all six object-environment interaction settings. Although MJX supports efficient gradient-based parameter estimation, its applicability is restricted to simple meshes (typically fewer

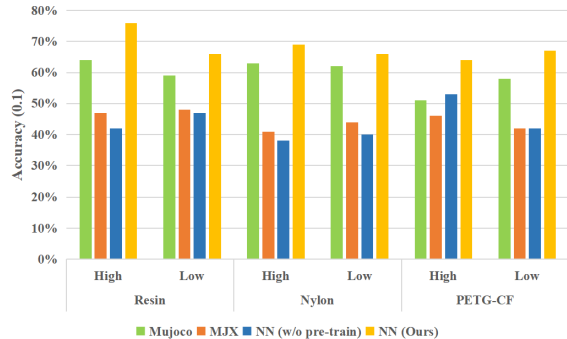


Fig. 4: Collision model accuracy ($\alpha = 0.1$) in different settings. Our fine-tuned strategy effectively avoids overfitting on scarce real-world data and achieves higher accuracy than MuJoCo, whose performance is limited by unmodeled effects.

TABLE II: Collision Model Accuracy($\alpha = 0.1$) For Three Shape Blocks.

Method	Semi-Cylinder	Square	Triangle
MuJoCo	0.64	0.50	0.49
NN(w/o Pre-train)	0.42	0.42	0.36
NN(ours)	0.76	0.55	0.54

than 20 vertices) due to stability constraints in gradient computation. Simplifying the semi-cylinder to satisfy this requirement significantly alters its geometry, resulting in large discrepancies between simulated and real-world collisions. In contrast, our surrogate model, implemented as a three-layer MLP, avoids gradient instability and can identify collision-related parameters for complex meshes. The third baseline that directly trains on the small real-world dataset suffers from severe overfitting and poor generalization. By pre-training on large-scale simulation data and fine-tuning with limited real interactions, our model achieves substantially higher prediction accuracy and better captures the underlying collision dynamics.

TABLE III: Error in Model-Based Optimization

Simulator	Semi-Cylinder		Square		Triangle	
	Pos/m	Ori/rad	Pos/m	Ori/rad	Pos/m	Ori/rad
MuJoCo	0.0245(± 0.0176)	0.7882(± 0.6071)	0.0222(± 0.0124)	1.2696(± 0.6926)	0.0251(± 0.0154)	0.6673(± 0.4036)
Hybrid Simulator (w/o Pre-train)	0.0363(± 0.0156)	0.5751(± 0.5074)	0.0243(± 0.0140)	1.9751(± 0.8621)	0.0303(± 0.0187)	0.7027(± 0.5069)
Hybrid Simulator (Ours)	0.0159(± 0.0046)	0.4152(± 0.3014)	0.0163(± 0.0080)	1.2479(± 1.0630)	0.0185(± 0.0092)	0.7319(± 0.5518)

TABLE IV: Time Cost in CMA-ES

Time(s)	Semi-cylinder	Square	Triangle
MuJoCo	27.42(± 3.24)	28.58(± 3.71)	25.20(± 2.89)
Hybrid Simulator (Ours)	15.81(± 2.75)	14.74(± 1.83)	13.21(± 3.52)

B. Model-Based Optimization

After obtaining an accurate collision model, we integrate it into the physics engine to construct the hybrid simulator. The hybrid simulator employs the learned model to simulate collision outcomes, while relying on MuJoCo for other dynamics.

1) *Experiment Setup*: In this task, we randomly select target positions and orientations, and use the simulator to search for the optimal impact point and velocity. The resulting parameters are then executed on the Franka arm in real, where we measure the distance and orientation errors between the actual and desired outcomes. We evaluate performance on three different object shapes (semi-cylinder, square, and triangle), as illustrated in Fig. 6a.

2) *Methods and Metrics*: Due to gradient instability in long-horizon simulations and collisions involving complex meshes, we exclude MJX from the baseline comparisons. Instead, we evaluate three settings: (i) pure MuJoCo, (ii) a hybrid simulator with a collision model trained only on the real-world dataset, and (iii) a hybrid simulator with the collision model trained using our proposed CLASH framework. Given sampled target positions and orientations, we adopt CMA-ES[28], a widely used derivative-free optimization algorithm, to search for the optimal impact point and velocity that minimizes a combined position-orientation error:

$$\mathcal{L}_{search} = \|\text{Pos}_{pred} - \text{Pos}_{target}\|^2 + \tau \|\text{Ori}_{pred} - \text{Ori}_{target}\|^2 \quad (5)$$

where τ is a weighting factor to balance the importance of position and orientation accuracy. In practice, we set $\tau = 0.01$ to bring the two errors into a comparable scale. The optimized impact parameters are then converted into Cartesian velocity control commands executed on the Franka arm. For each shape, we randomly sample five target poses (position and orientation) and repeat the experiment five times per target. We report the mean and standard deviation of both position error and orientation error across all trials.

3) *Results*: To build the hybrid simulators, we first follow the procedure described in Section IV-A to obtain collision models for each block shape. The accuracy of these models is summarized in Table II. We then integrate the learned collision models with MuJoCo and evaluate the resulting

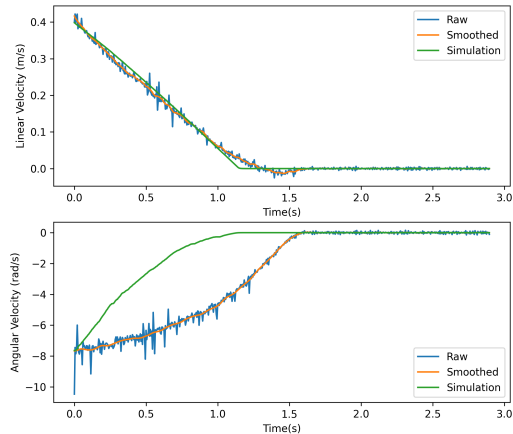


Fig. 5: Linear and angular velocities of the square block in simulation and real world. MuJoCo captures the linear velocity decay reasonably well, but fails to reproduce the angular velocity decay accurately. Raw: raw measurements from the real world. Smoothed: filtered real-world data. Simulation: MuJoCo-simulated data.

hybrid simulators, reporting the mean error (\pm standard deviation) in Table III. Across all shapes, our method achieves a substantial reduction in positioning error: 35.10% for the semi-cylinder, 26.58% for the square, and 26.29% for the triangle. While achieving high accuracy in positioning, we observe that orientation errors for the square and triangular blocks remained large. We attribute this limitation primarily to the inaccurate modeling of torsional friction for these geometries, as illustrated in Fig. 5. A potential remedy would be to introduce an improved friction model, which we leave for future work. In addition to accuracy, we also evaluate efficiency. Table IV reports the average runtime and standard deviation of CMA-ES optimization with and without our collision model. By representing the collision process with our learned model, the hybrid simulator substantially reduces optimization time, meanwhile achieving higher simulation fidelity.

C. RL With Hybrid Simulator

1) *Experiment Setup*: We further evaluate the hybrid simulator in a reinforcement learning (RL) task. The objective is to push a semi-cylinder from a starting point to an end point without leaving the designated area (Fig. 6b). This task poses two main challenges. First, it requires accurate modeling of

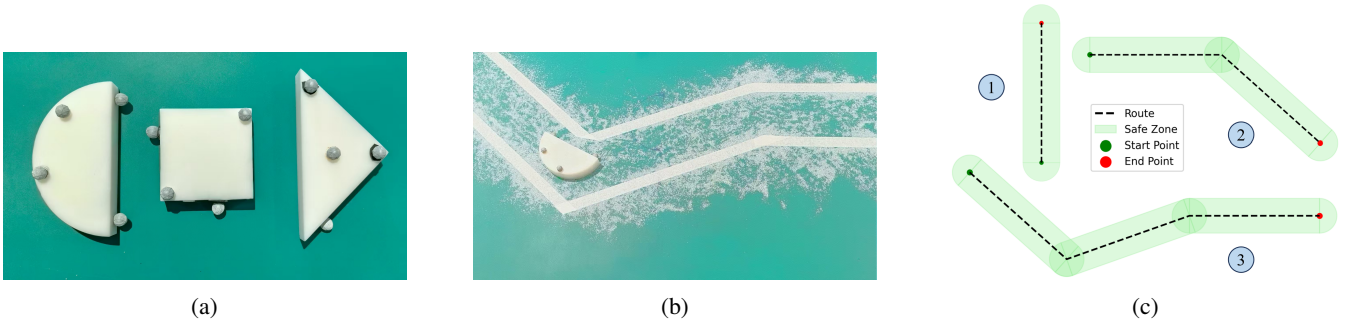


Fig. 6: (a) The three block shapes used in the model-based optimization experiments: semi-cylinder, square, and triangle (from left to right). (b) The designated workspace, bounded by the two white lines. (c) The three evaluation routes used in the RL experiments. The difficulty increases from Route 1 to Route 3. For Route 1 and 2, the initial orientation of the semi-cylinder is randomized, while for Route 3 it is fixed.

TABLE V: Reward function design for policy learning. The total reward is $R = R_1 + R_2 + R_3 + R_4$.

Term	Formula	Description
R_1	$\exp(-\Delta x^2)$	Dense position reward
R_2	$(1 + \cos(\Delta\theta))/2$	Orientation reward at sub-goal
R_3	$T - t$	Strike efficiency reward at sub-goal
R_4	r_0	Penalty for leaving safe zone

both collision and sliding, as even a single strike can cause the object to leave the safe zone, despite appearing stable in simulation. Second, only impacts on the arc side of the semi-cylinder are permitted (Fig. 3b). If the arc is misaligned with the target direction, the strike will fail to move the object toward its destination. Consequently, orientation must be explicitly considered in the reward design. We evaluate the trained policies on routes of three different shapes (Fig. 6c).

2) *Method and Metrics*: We adopt a hierarchical formulation for training efficiency and composability: short straight segments are easier to learn, and arbitrarily long or diverse paths can be formed by concatenating segments. So we only train a low-level collision policy to finish one straight segment at a time. A high-level planner updates the sub-goal (position and orientation) at each segment boundary. The route is partitioned into straight segments of 0.3×0.08 m. A sub-goal is declared reached when the semi-cylinder is within 0.04 m of the target point. Upon completion, the next sub-goal position is set to the end of the upcoming segment, and its orientation aligns with the direction from the next sub-goal position to the one after it. This design reduces credit-assignment difficulty on long horizons while enabling straightforward path composition.

We train the sub-goal policy using Soft Actor-Critic (SAC) in two environments: MuJoCo and our hybrid simulator. Policies are trained for 200,000 steps using the Stable-Baselines3[30] implementation, with default hyperparameters. The observation space includes the absolute position of the semi-cylinder and the relative position and orientation of the sub-goal. The action space specifies the

TABLE VI: Results in Sequential Semi-Cylinder Pushing Task

Simulator	Route 1	Route 2		Route 3	
	SR	SR	SGCR	SR	SGCR
MuJoCo	4/10	2/10	8/20	1/10	13/30
Hybrid Simulator (ours)	8/10	5/10	14/20	5/10	21/30

impact point and velocity of the striking block. To guide policy learning, we design a reward function that balances position accuracy, orientation alignment, strike efficiency, and safety. The reward terms are summarized in Table V. Specifically, R_1 provides a dense signal based on the distance Δx to the sub-goal, while R_2 and R_3 give sparse rewards upon reaching the sub-goal. Here, $\Delta\theta$ denotes the orientation deviation, t is the number of strikes used in the sub-task, and T is the maximum strikes allowed. R_4 penalizes the agent if the semi-cylinder leaves the designated safe zone. This design combines dense feedback for stable learning with sparse, goal-related signals to enforce correct orientation and strike efficiency. In practice, we set $T = 5$ and $r_0 = -10$.

Each path is tested ten times with the same low level policy. We report both the success rate (SR), defined as the fraction of trials in which the full path is completed, and the sub-goal completion rate (SGCR), defined as the ratio of successfully completed segments to the total number of segments.

3) *Results*: The results are summarized in Table VI. The policies trained with the hybrid simulator achieve consistently higher SR and SGCR compared to those trained with MuJoCo alone. This demonstrates that the hybrid simulator provides more accurate collision predictions, leading to policies that transfer more reliably to the real world. These findings confirm the importance of accurate collision modeling in narrowing the sim-to-real gap for RL tasks.

V. CONCLUSIONS AND DISCUSSIONS

In summary, CLASH provides a novel framework to integrate simulation and real-world data for complex dynamics modeling. By first distilling physics priors from conventional

simulators to differentiable surrogate base models, and then augmenting them with a minimal set of real world data, CLASH creates a hybrid simulator of both higher physical fidelity and faster computation, breaking the conventional trade-off between accuracy and speed. More importantly, CLASH demonstrates a scalable pathway for enhancing physics simulators by selectively replacing inaccurate components with data-driven models, paving the way for more reliable sim-to-real transfer.

Building on this foundation, our work opens a few avenues for future research. One promising direction is to extend the CLASH to other challenging physical processes where existing simulators like MuJoCo exhibit modeling discrepancies, such as the torsional friction effects observed in our experiments. Reducing the accuracy dependency on the fidelity of the underlying simulator is also worth exploring. Furthermore, to broaden the framework’s applicability to novel objects without retraining, future work will explore incorporating scalable geometric representations into the surrogate model. Integrating inputs like point clouds could enable generalization across diverse object geometries, representing a key step towards a general-purpose data-driven simulator.

REFERENCES

- [1] W. Zhao, J. P. Queralta, and T. Westerlund, “Sim-to-real transfer in deep reinforcement learning for robotics: a survey,” in *2020 IEEE Symposium Series on Computational Intelligence (SSCI)*. IEEE, 2020, pp. 737–744.
- [2] E. Todorov, T. Erez, and Y. Tassa, “Mujoco: A physics engine for model-based control,” in *2012 IEEE/RSJ international conference on intelligent robots and systems*. IEEE, 2012, pp. 5026–5033.
- [3] N. Corporation, “Isaac lab documentation,” <https://isaac-sim.github.io/IsaacLab/>, 2024, accessed: Sep. 3, 2024.
- [4] J. Schulman, F. Wolski, P. Dhariwal, A. Radford, and O. Klimov, “Proximal policy optimization algorithms,” *arXiv preprint arXiv:1707.06347*, 2017.
- [5] T. Haamoja, A. Zhou, P. Abbeel, and S. Levine, “Soft actor-critic: Off-policy maximum entropy deep reinforcement learning with a stochastic actor,” in *International conference on machine learning*. Pmlr, 2018, pp. 1861–1870.
- [6] T. A. Howell, S. Le Cleac’h, J. Z. Kolter, M. Schwager, and Z. Manchester, “Dojo: A differentiable simulator for robotics,” *arXiv preprint arXiv:2203.00806*, vol. 9, no. 2, p. 4, 2022.
- [7] E. Coumans and Y. Bai, “Pybullet, a python module for physics simulation for games, robotics and machine learning,” 2016.
- [8] “NVIDIA PhysX SDK,” <https://developer.nvidia.com/physx-sdk>, accessed: 2025-09-09.
- [9] R. Tedrake *et al.*, “Drake: Model-based design and verification for robotics,” 2019.
- [10] K. Werling, D. Omens, J. Lee, I. Exarchos, and C. K. Liu, “Fast and feature-complete differentiable physics for articulated rigid bodies with contact,” *arXiv preprint arXiv:2103.16021*, 2021.
- [11] M. Memmel, A. Wagenmaker, C. Zhu, P. Yin, D. Fox, and A. Gupta, “Asid: Active exploration for system identification in robotic manipulation,” *arXiv preprint arXiv:2404.12308*, 2024.
- [12] P. Y. Chen, C. Liu, P. Ma, J. Eastman, D. Rus, D. Randle, Y. Ivanov, and W. Matusik, “Learning object properties using robot proprioception via differentiable robot-object interaction,” *arXiv preprint arXiv:2410.03920*, 2024.
- [13] L. Shi, Y. Xu, S. Wang, J. Huang, W. Zhao, Y. Jia, Z. Yan, W. Gu, and G. Zhou, “An real-sim-real (rsr) loop framework for generalizable robotic policy transfer with differentiable simulation,” *arXiv preprint arXiv:2503.10118*, 2025.
- [14] B. Wang, X. Meng, X. Wang, Z. Zhu, A. Ye, Y. Wang, Z. Yang, C. Ni, G. Huang, and X. Wang, “Embodiedreamer: Advancing real2sim2real transfer for policy training via embodied world modeling,” *arXiv preprint arXiv:2507.05198*, 2025.
- [15] J. Tobin, R. Fong, A. Ray, J. Schneider, W. Zaremba, and P. Abbeel, “Domain randomization for transferring deep neural networks from simulation to the real world,” in *2017 IEEE/RSJ international conference on intelligent robots and systems (IROS)*. IEEE, 2017, pp. 23–30.
- [16] K. Bousmalis, A. Irpan, P. Wohlhart, Y. Bai, M. Kelcey, M. Kalakrishnan, L. Downs, J. Ibarz, P. Pastor, K. Konolige, *et al.*, “Using simulation and domain adaptation to improve efficiency of deep robotic grasping,” in *2018 IEEE international conference on robotics and automation (ICRA)*. IEEE, 2018, pp. 4243–4250.
- [17] E. Heiden, D. Millard, E. Coumans, Y. Sheng, and G. S. Sukhatme, “Neuralsim: Augmenting differentiable simulators with neural networks,” in *2021 IEEE International Conference on Robotics and Automation (ICRA)*. IEEE, 2021, pp. 9474–9481.
- [18] J. Gao, M. Y. Michelis, A. Spielberg, and R. K. Katzschmann, “Sim-to-real of soft robots with learned residual physics,” *IEEE Robotics and Automation Letters*, 2024.
- [19] A. Ajay, J. Wu, N. Fazeli, M. Bauza, L. P. Kaelbling, J. B. Tenenbaum, and A. Rodriguez, “Augmenting physical simulators with stochastic neural networks: Case study of planar pushing and bouncing,” in *2018 IEEE/RSJ International Conference on Intelligent Robots and Systems (IROS)*. IEEE, 2018, pp. 3066–3073.
- [20] N. Fazeli, S. Zapolsky, E. Drumwright, and A. Rodriguez, “Learning data-efficient rigid-body contact models: Case study of planar impact,” in *Conference on Robot Learning*. PMLR, 2017, pp. 388–397.
- [21] G. Authors, “Genesis: A universal and generative physics engine for robotics and beyond,” [URL https://github.com/Genesis-Embodied-AI/Genesis](https://github.com/Genesis-Embodied-AI/Genesis), 2024.
- [22] H. Geng, F. Wang, S. Wei, Y. Li, B. Wang, B. An, C. T. Cheng, H. Lou, P. Li, Y.-J. Wang, *et al.*, “Roboverse: Towards a unified platform, dataset and benchmark for scalable and generalizable robot learning,” *arXiv preprint arXiv:2504.18904*, 2025.
- [23] DeepMind, “Mjx: Jax-accelerated mujoco,” <https://mujoco.readthedocs.io/en/stable/mjx.html>, 2024, accessed: Sep. 3, 2024.
- [24] M. Macklin, “Warp: A high-performance python framework for gpu simulation and graphics,” <https://github.com/nvidia/warp>, March 2022, nVIDIA GPU Technology Conference (GTC).
- [25] K. M. Jatavallabhula, M. Macklin, F. Golemo, V. Voleti, L. Petrini, M. Weiss, B. Considine, J. Parent-Lévesque, K. Xie, K. Erleben, *et al.*, “gradsim: Differentiable simulation for system identification and visuomotor control,” *arXiv preprint arXiv:2104.02646*, 2021.
- [26] F. Golemo, A. A. Taiga, A. Courville, and P.-Y. Oudeyer, “Sim-to-real transfer with neural-augmented robot simulation,” in *Conference on Robot Learning*. PMLR, 2018, pp. 817–828.
- [27] P.-T. De Boer, D. P. Kroese, S. Mannor, and R. Y. Rubinstein, “A tutorial on the cross-entropy method,” *Annals of operations research*, vol. 134, no. 1, pp. 19–67, 2005.
- [28] N. Hansen, “The cma evolution strategy: A tutorial,” *arXiv preprint arXiv:1604.00772*, 2016.
- [29] I. Loshchilov and F. Hutter, “Decoupled weight decay regularization,” *arXiv preprint arXiv:1711.05101*, 2017.
- [30] A. Raffin, A. Hill, A. Gleave, A. Kanervisto, M. Ernestus, and N. Dormann, “Stable-baselines3: Reliable reinforcement learning implementations,” *Journal of Machine Learning Research*, vol. 22, no. 268, pp. 1–8, 2021. [Online]. Available: <http://jmlr.org/papers/v22/20-1364.html>